Since January 2020 Elsevier has created a COVID-19 resource centre with free information in English and Mandarin on the novel coronavirus COVID-19. The COVID-19 resource centre is hosted on Elsevier Connect, the company's public news and information website.

Vaccine 40 (2022) 5529–5536

Contents lists available at ScienceDirect

Vaccine

journal homepage: www.elsevier.com/locate/vaccine

Functional profiling of Covid 19 vaccine candidate by flow virometry

Ashley Prout [a], Richard R. Rustandi [a], Christopher Tubbs [a], Michael A. Winters [b], Philip McKenna [c], Josef Vlasak [a,*]

[a] Vaccine Analytical Research and Development, Merck & Co., Inc., West Point, PA, USA
[b] Vaccine Process Research and Development, Merck & Co., Inc., West Point, PA, USA
[c] Infectious Diseases-Vaccines, Merck & Co., Inc., West Point, PA, USA

ARTICLE INFO

Article history:
Received 16 November 2021
Received in revised form 20 May 2022
Accepted 3 August 2022
Available online 9 August 2022

Keywords:
Covid 19 vaccine
Flow virometry
SARS-CoV-2 spike protein
Vesicular stomatitis virus
Vaccine development

ABSTRACT

Vaccine development is a complex process, starting with selection of a promising immunogen in the discovery phase, followed by process development in the preclinical phase, and later by clinical trials in tandem with process improvements and scale up. A large suite of analytical techniques is required to gain understanding of the vaccine candidate so that a relevant immunogen is selected and subsequently manufactured consistently throughout the lifespan of the product. For viral vaccines, successful immunogen production is contingent on its maintained antigenicity and/or infectivity, as well as the ability to characterize these qualities within the context of the process, formulation, and clinical performance. In this report we show the utility of flow virometry during preclinical development of a Covid 19 vaccine candidate based on SARS-CoV-2 spike (S) protein expressed on vesicular stomatitis virus (VSV). Using a panel of monoclonal antibodies, we were able to detect the S protein on the surface of the recombinant VSV virus, monitor the expression levels, detect differences in the antigen based on S protein sequence and after virus inactivation, and monitor S protein stability. Collectively, flow virometry provided important data that helped to guide preclinical development of this vaccine candidate.

1. Introduction

Flow virometry is an emerging technique that is opening new avenues for studying viruses and extracellular vesicles [1,2]. This technique allows for the enumeration and detailed characterization of particles using both their light-scattering characteristics and molecular markers, such as nucleic acids or specific protein antigens [3,4]. The ability to employ specific antibodies allows these methods to address a variety of different questions, including protein maturation state [5] or conformation [6–8].

Coronavirus disease 2019 (Covid 19), caused by the severe acute respiratory syndrome coronavirus 2 (SARS-CoV-2) has swiftly spread across the world and became the most severe pandemic in recent history. An unprecedented worldwide effort has led to rapid development of several highly efficacious vaccines [9] and the development of additional vaccines continues [10]. The vaccines are based on viral Spike (S) protein, which mediates binding to target cells and subsequent fusion. Coronavirus S protein is a class I fusion protein [11] arranged into homotrimers on the viral surface. The protein is expressed in a metastable prefusion conformation [12], which is the main target of neutralizing antibodies [13,14]. The structure of the pre-fusion trimer was determined by cryo-transmission electron microscopy [15]. S protein consists of two functional subunits, S1 and S2. The S1 subunit contains the receptor-binding domain (RBD), while the S2 subunit contains the viral fusion machinery and the membrane anchor. SARS-CoV-2, but not other SARS-like viruses, has evolved a multi basic cleavage site at the S1-S2 boundary [16]. Cleavage of the multi basic site by furin primes the S protein for fusion and is thought to be responsible for the high infectivity of SARS-CoV-2 relative to related Coronaviruses. Human angiotensin-converting enzyme 2 (hACE2) serves as the receptor for SARS-CoV-2 [16]. Upon receptor binding, the cellular serine protease TMPRSS2 is recruited to cleave S protein at a S2′ cleavage site, which exposes the fusion peptide and subsequently leads to fusion [17]. Stabilization of the metastable prefusion conformation is essential for the development of S protein-based vaccines. This has largely been achieved by introducing two consecutive proline residues (2P) in the loop between the first heptad repeat and the central helix [15,18].

For a successful development of a new vaccine, detailed understanding of the immunogen is essential. However, due to the complexity of viral vaccines, achieving in-depth analytical

* Corresponding author.
E-mail address: josef_vlasak@merck.com (J. Vlasak).

https://doi.org/10.1016/j.vaccine.2022.08.006
0264-410X/

understanding of the sample is challenging and new methods are needed to accelerate vaccine development. In this report, we show the application of flow virometry to characterize a Covid 19 vaccine candidate produced from a recombinant VSV viral vector expressing SARS-CoV-2 S protein. Our data demonstrate that flow virometry is a powerful tool for monitoring critical attributes of viral samples throughout all stages of viral vaccine development, including antigen selection in the discovery phase, process development in the pre-clinical stage, and product quality monitory in later stages. Additionally, the relatively short time required for data acquisition makes flow virometry amenable for real-time process monitoring as a part of Process Analytical Technology (PAT) toolbox.

2. Material and methods

2.1. Vaccine candidate preparation

Replication-competent, chimeric virus (VSV△G-SARS-CoV-2) was generated by replacing the VSV glycoprotein (G) gene with a coding sequence for the SARS-CoV-2 S protein. The S protein sequence contained the 2P prefusion stabilization, as well as several additional mutations (Table 1). VSV△G-SARS-CoV-2 virus was produced in Vero cells in buffered serum-free medium VP-SFM (ThermoFisher Scientific). Medium from infected cell cultures was harvested and clarified using a Sartoclean® CA 3 μm/0.8 μm filter (Sartorius). An endonuclease was added to digest Vero host cell nucleic acid. Clarified virus fluid was purified using Capto™-Core 700 chromatography (Cytiva). Virus product from the Capto-Core column was further purified using hollow fiber, tangential flow ultrafiltration. The virus, retained by the hollow fiber membrane, was concentrated and diafiltered against 10 mM Tris buffer with sucrose (0–10% w/v) and sodium chloride (0–150 mM).

2.2. Pseudotyped HIV-1 preparation

Pseudotyped lentiviral particles carrying SARS-CoV-2 S protein were generated via a two-plasmid transfection into Lenti-X 293 T cells (Takarabio). Briefly, the coding sequence for SARS-CoV-2 S protein carrying a C-terminal truncation of the final 18 residues was cloned into mammalian expression vector pV1Jns [19]. This plasmid was co-transfected with an envelope-deleted genomic lentiviral plasmid containing a GFP reporter. Transfections were carried out according to manufacturer's recommendations (Fugene6, Promega). 48 h post transfection, supernatant virus was collected, clarified (5 min spin at 1200 rpm) and pseudovirus particles were concentrated by LentiX concentrator (Takarabio) according to manufacturer's recommendations.

2.3. Cryo transmission electron microscopy (cryo-TEM)

Electron microscopy was performed using an FEI Tecnai T12 electron microscope, operating at 120 keV equipped with an FEI Eagle 4 k × 4 k CCD camera. A 3 μL drop of the sample was applied on a holey carbon copper grid, blotted away with a filter paper, and immediately vitrified in liquid ethane. Vitreous ice grids were transferred into the electron microscope using a cryostage that maintains the grids at a temperature below −170 °C.

2.4. Flow virometry

Viral handling was performed in biosafety level 2 laboratories. The Apogee A50 Micro flow cytometer (Apogee Flow Systems, Hemel Hempstead, UK) was equipped with a variable output 405 nm laser (up to 300 mW) used for light scattering and a 200 mW 488 nm laser used for fluorescence. The instrument was set to trigger on side light scattering (SSC). The sheath fluid pressure was set at 150 mbar and samples were introduced at a flow rate of 1.5 μL/min. Particle concentration of $2x10^8$ particles/ml was targeted for measurement. To ensure that only particles present in the sample were being detected, system suitability check was performed prior to every run: 1) the instrument was thoroughly cleaned sequentially by 1% bleach, flow cell cleaning fluid (Apogee Flow Systems), and buffer until the concentration of particles detected in the buffer blank was less than $2x10^6$ particles/ml (i.e. 100x less than the targeted sample particle concentration); 2) the electronics noise peak was identified in a buffer blank with a clean system and the threshold was then set to exclude the electronics noise from the data.

2.5. Flow virometry antibody labelling

Sample particle concentration was first determined by flow virometry and then diluted with phosphate buffered saline (PBS) to $1x10^9$ particles/mL for each antibody labeling reaction. 100 μL of the sample was mixed with 1 μL (typically at about 1 mg/mL) of the primary anti-S antibody (Table 2) and incubated for 1 h at room temperature. After incubation the unbound primary antibody was removed using Capto™Core 700 resin (Cytiva) – a small spin column with about 1 cm bed height was prepared and equilibrated with PBS. The sample was spun for 30 s at 500 g through the column. Cleaned up sample was incubated with 3 μL (typically at about 1 mg/mL) of secondary antibody (Table 3) labeled with AlexaFluor 488 (Thermo Fisher Scientific) for 1 h in the dark at room temperature. After incubation the unbound secondary antibody was removed the same way as the unbound primary antibody. The sample was then diluted 5x in PBS buffer and measured by the flow cytometer. Samples stained with only the secondary antibody (no primary Ab) were used as controls.

2.6. Simple Western™ blotting

For the western blot analysis, the capillary-based Simple Western™ technology (ProteinSimple) was used. In this technique the sample is separated by size in a capillary, followed by immobilization, labeling, and detection directly in the capillary. The samples were appropriately diluted with 1X sample buffer (ProteinSimple). Each sample was mixed 1:1 with 2X master mix (20 μL 10X sample buffer, one vial master mix, 20 μL 0.8 M DTT, 60 μL water). The mixture was vortexed and heated at 90 °C for 10 min, cooled down at room temperature, and spun down. Sample mixtures were then added into wells of Simple Western™ plates and analyzed according to manufacturer's manual with chemiluminescent detection

Table 1
Sequence characteristics of the vaccine candidate and the 2P construct also evaluated in early development.

Construct	2P Prefusion Stabilization	Furin Site ^{682}RRAR^{685}	Cytoplasmic tail	Other mutation
WT S protein		YQTQTNSP**RRAR**S		
2P construct	K986P/V987P	YQTQTNSP**RRAR**S	(△18 deletion)	
vaccine candidate	K986P/V987P	YQTQTNSP**RGAR**S	(△23 deletion)	S813F

Table 2
Panel of Primary Antibodies and a Fusion Protein (Fc) Utilized for Flow Virometry.

Catalog number	Manufacturer	Immunogen	Neutralizing	Species
human ACE2-Fc (AC2-H5257)	Acro Biosystems	N/A	Yes	Human
AM91337	Active Motif	S1	No	Human
AM91339	Active Motif	S1	No	Human
AM91341	Active Motif	S1	No	Human
AM91347	Active Motif	S1	No	Human
AM91349	Active Motif	S1	Yes	Human
AM91351	Active Motif	S1	No	Human
AM91361	Active Motif	S1	Yes	Human
40150-D003	Sino Biological	RBD	Unknown	Mouse
40591-MM43	Sino Biological	S1-mFc aa16-685	Yes	Mouse
40592-R001	Sino Biological	RBD-mFc Protein	Yes	Rabbit
GTX135356	GeneTex	S1 N-term. region	Unknown	Rabbit
GTX632604	GeneTex	S2 aa 1029–1192	Unknown	Mouse
MP8720411	MP Biomedicals	S2 (B)	Yes	Mouse
MP8720301	MP Biomedicals	S1	Unknown	Mouse

RBD – receptor binding domain.

Table 3
Secondary Antibodies Utilized for Flow Virometry and Simple Western.

Method	Secondary	Catalog number	Manufacturer	Species
Flow virometry	Anti-human	709-545-149	Jackson ImmunoResearch Laboratories Inc.	Donkey
Flow virometry	Anti-mouse	A21202	Invitrogen	Donkey
Flow virometry	Anti-rabbit	711-545-152	Jackson ImmunoResearch Laboratories Inc.	Donkey
Simple Western	Anti-rabbit	042-206	Protein Simple	Proprietary, unlisted

using primary antibodies (Table 4) and a secondary antibody conjugated to horseradish peroxidase (Table 3). Linear response range between the western blot signal and sample dilution was established and samples were tested within this range. Further details of the validated anti-spike assay will be described elsewhere (Gillespie et al., manuscript in preparation).

2.7. Virus pelleting

Pelleting conditions were established by measuring remaining virus particles in the supernatant after sedimentation at 16,000 g for varying time. 30 min at 16,000 g was selected as the condition that pelleted more than 90% of particles measured by flow virometry in 100 μL of sample. After pelleting, 95 μL of the supernatant were withdrawn and the pellet was resuspended in 95 μL of PBS. Both fractions were then analyzed by a Simple Western™.

3. Results and discussion

3.1. Detection of VSV virus particles by flow virometry

VSV is a morphologically uniform, bullet-shaped virus of approximately 70 × 200 nm [20] (Fig. 1, left panel), sufficiently large to be detectable by light scattering using flow virometry [21]. To confirm that the detected particles were indeed particles present in the sample, two control measurements were conducted. First, a clean buffer and a sample were run with a trigger threshold set to low values to reveal electronics noise from the instrument. The data showed that the particles in the sample were well separated from the electronics noise of the instrument (Fig. 1, right panel, top). Second, particle concentration in the buffer control, with the threshold set to exclude electronics noise, was compared to particle concentration detected in the sample (Fig. 1, right panel, bottom). This comparison showed that particle concentration in the buffer control was negligible (less than 1%) compared to particle concentration detected in the sample. For routine analysis, the threshold was set such that only true particles were being detected and the concentration of particles shed by the instrument was controlled by cleaning the instrument before use. The narrow light-scattering peak observed by flow virometry, consistent with the monodisperse population of VSV virions, suggested high purity of the sample, which was confirmed by cryo-TEM analysis that showed most particles in the samples were VSV virions (Fig. 1, left panel).

Table 4
Primary Antibodies Utilized for Simple Western.

Catalog number	Manufacturer	Immunogen	Species
40592-T62	Sino Biological	Recombinant SARS-CoV-2/ 2019-nCoV Spike/RBD Protein	Rabbit
40590-T62	Sino Biological	Recombinant SARS-CoV-2/ 2019-nCoV Spike/S2 Protein	Rabbit
REA005	Imanis Life Sciences	Purified stock of VSV-hIFNβ virus for nucleoprotein (N)	Rabbit

3.2. Detection of S protein on virus particles by flow virometry

The identity of particles observed by flow virometry was further confirmed by S-protein detection on the particles. The samples were stained with an antibody specific for the S protein or with the chimeric S-protein receptor ACE2 fused to human antibody Fc fragment to allow detection with anti-human secondary antibodies (Fig. 2, top panel, left). The result demonstrated the presence of S-protein bearing particles among the particle pool, although with a variable degree of labeling. In addition, about half of the particles in the sample appeared negative for the S protein but had the narrow light scattering signal that would be expected for the monodisperse population of VSV virions and not for extracellular vesicles or protein aggregates that are typically polydisperse. It is likely that at least some of the particles appearing negative in our assay still expressed the S protein, but the level was below the limit of detection. The varying density of S protein

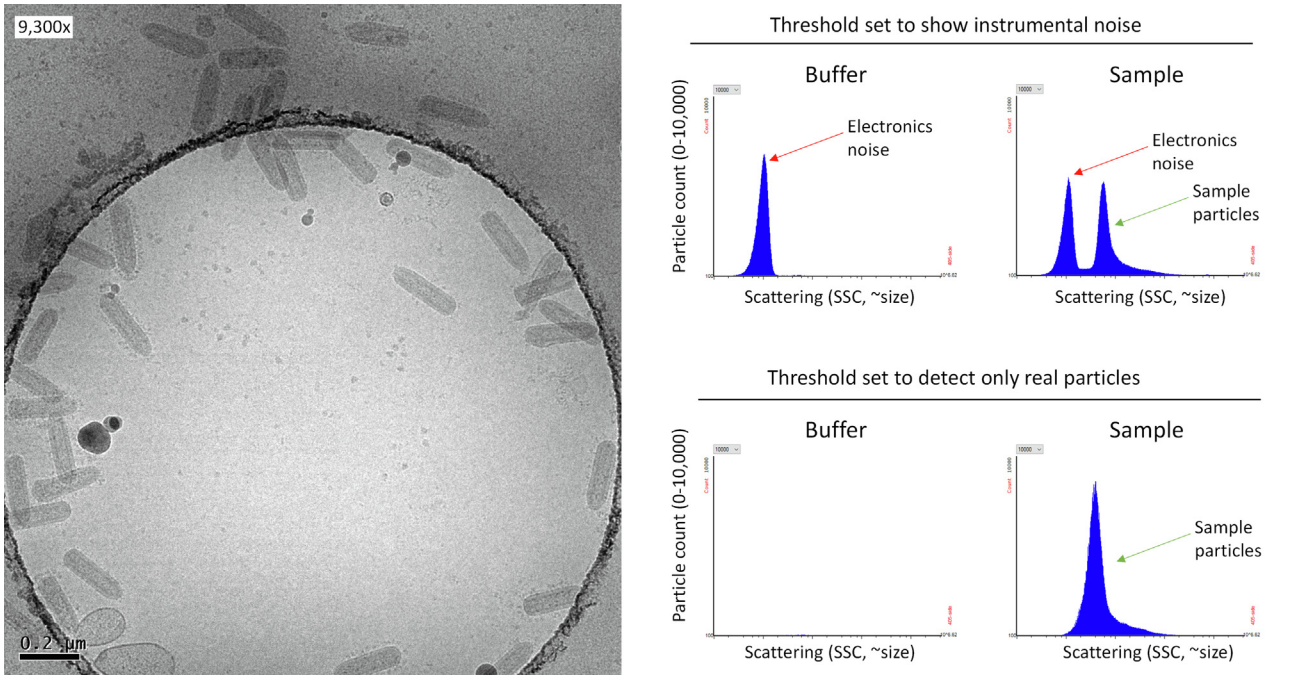

Fig. 1. Representative cryo-TEM image and flow virometry histograms. Left panel – cryo-TEM image. Right panel – side scatter (SSC) histograms scaled identically. Top right – examples of buffer and samples run with the threshold set to reveal electronics noise. Bottom right – a typical analysis, with the threshold set such that the electronics noise was excluded. Background particles present in the buffer control are negligible (not apparent in the buffer histogram). All data pictured was replicated across numerous independent runs.

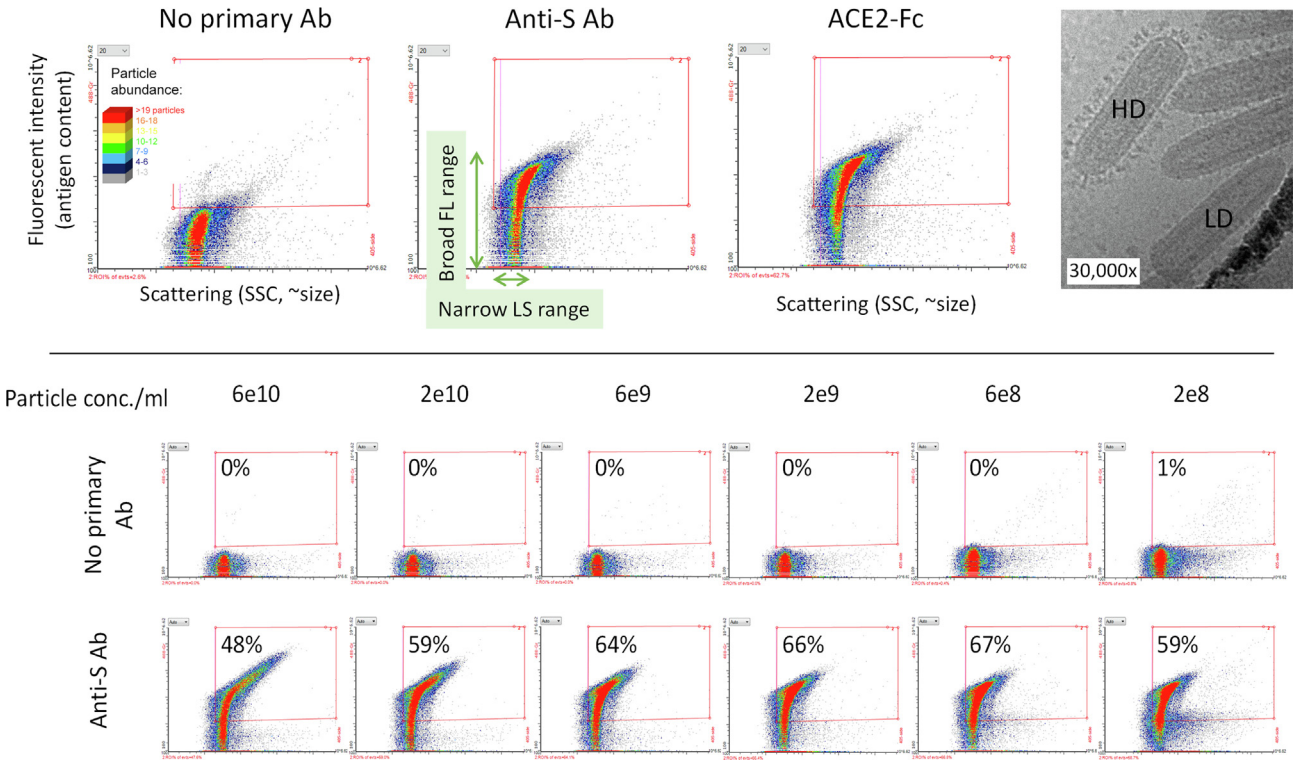

Fig. 2. S-protein detection of VSV virions by flow virometry. Top panel – three-dimensional scatter plots representing antigen content via fluorescence intensity (y-axis) versus SSC, with particle abundance (z-axis) depicted via a heatmap color scale (color scale indicated in the left panel). The gate for antigen-positive particles is drawn based on the control with no primary antibody. The broad fluorescence signal and the narrow LS signal of FL-negative particles are indicated with green arrows. Top right image, cryo-TEM image at 30,000x showing high S-protein density VSV particles (HD) and low S-protein density VSV particles (LD). Bottom panel – assessment of particle aggregation during antibody labelling. A series of sample concentrations was incubated with a constant concentration of antibodies and the % of S-protein positive particles was evaluated.

on VSV virions was also apparent in the cryo-TEM imaging (Fig. 2, top panel, right). Taken together, the data confirmed that the particles detected by flow virometry were predominantly monodisperse VSV virions but with a variable density of S protein on the surface.

Viral particles with high antigen density (high fluorescence intensity) also exhibited increased light scattering, which could suggest particle aggregation or swarming (two adjacent particles being detected as one larger particle). To address this concern, we have performed a 300-fold dilution series of the virus sample and labeled the samples with the same antibody concentrations (Fig. 2, bottom panel). Dilutions in the range of $6x10^8$ – $6x10^9$ particles/ml showed comparable light scattering signal after labeling with antibodies and comparable % of positive particles, while the samples at the higher concentrations (>$2x10^{10}$ particles/ml) showed an increased number of particles with greater light scattering signal and a reduced % of positive particles. This change in the profile at virus concentrations > 2×10^{10} particles/ml would indeed suggest an occurrence of aggregation and/or swarming but only at these high concentrations. Because the increased light scattering signal was not observed in the control series without the primary antibody, it could not have resulted from swarming of particles but was presumably mediated by the bivalent primary antibodies crosslinking individual virions. At the lowest virus concentration ($2x10^8$ particles/ml) there was an increased background in the form of mostly negative and large particles, which lowered the % of positive particles. These particles originated predominantly from the secondary antibody and were insignificant at higher virus concentrations.

Overall, this data confirmed that at the method's nominal virus concentration of $1x10^9$ particles/ml there was no significant aggregation and/or particle swarming. The increase in the light scattering signal is therefore attributed to the added mass on the virus particles as they are coated with the primary and secondary antibodies.

3.3. Monitoring S-protein expression levels

Flow virometry was utilized to evaluate S-protein expression of the vaccine candidate during development. In the early phase, differences in the S protein flow virometry signal were noted depending on the viral clone (Fig. 3, top panel). Similar changes were observed with multiple anti-S1 and anti-S2 antibodies, suggesting that the changes were due to different S-protein density on virus particles and not due to conformational changes in the protein. This was confirmed orthogonally using Simple Western blotting (Fig. 3, bottom panel) where the S protein is detected after denaturation and reduction and therefore protein conformation does not affect the signal. Quantification of the denatured S protein by Simple Western showed trends similar to those observed with quantification of the native S protein by flow virometry.

3.4. Binding studies with a panel of antibodies to evaluate epitopes of S protein variants and antigenicity after virus inactivation

An additional variant of the S protein was also considered during early vaccine development. This variant had the 2P mutation but the furin cleavage site was kept unchanged (Table 1). HIV-1 virus pseudotyped with the 2P variant was prepared and compared to the vaccine candidate using a panel of antibodies (Fig. 4). For each antibody, the percentage of antigen-positive particles between variants could be impacted by both the S-protein epitopes and quantity. If the epitopes were the same between variants, then the ratio of the % positive particles between them would be identical across antibodies because it would only reflect quantity. The result of this experiment, however, showed different ratios, which could be divided into three groups – for most antibodies, the 2P construct showed higher signal than the vaccine candidate (Fig. 4, blue bars), for four antibodies the 2P construct showed lower signal compared to the vaccine candidate (Fig. 4, yellow bars), and for one antibody the signals were reversed (Fig. 4, green

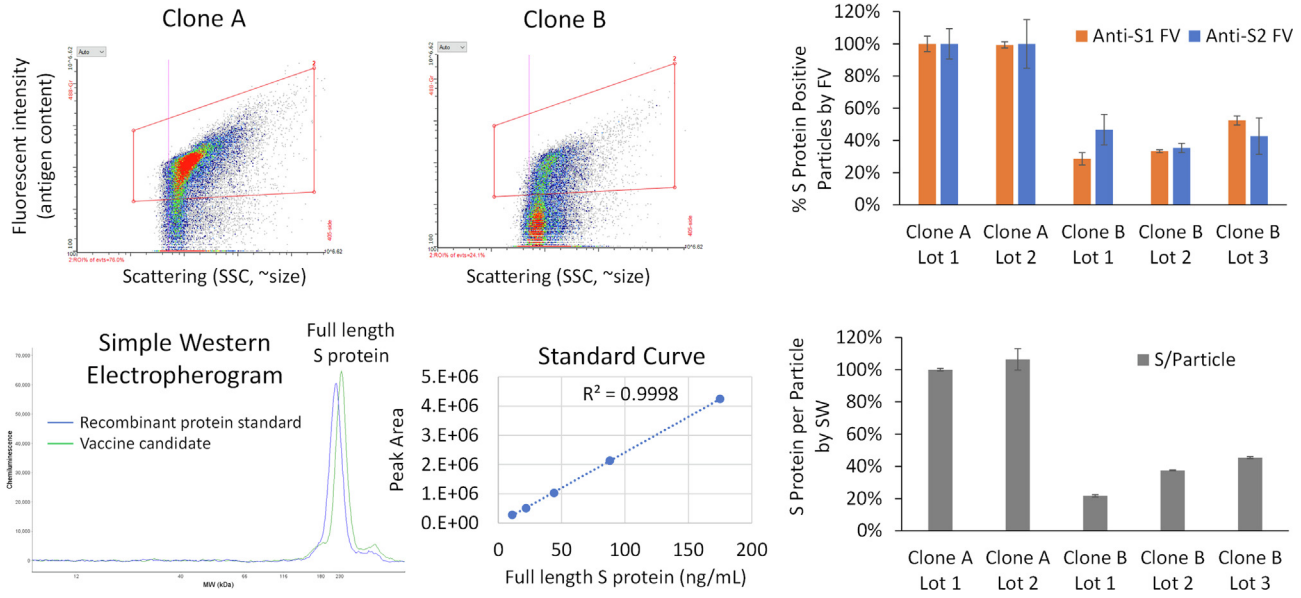

Fig. 3. S-protein quantification in vaccine candidate samples across clones and lots. Top panel from left to right – representative examples of flow virometry data (stained with AM91351 anti-S1 antibody) showing a sample with high S-protein expression (clone A) and a sample with low S-protein expression (clone B). Flow virometry (FV) quantification of anti-S1 (orange bars) and anti-S2 (blue bars) normalized to clone A lot 1 for ease of comparison. Error bars indicate standard deviations from duplicate independent runs. Bottom panel from left to right– example of a Simple Western (SW) electropherogram generated using a recombinant S protein (without the transmembrane domain) and a representative vaccine candidate sample, a 5-point standard curve generated with the recombinant S protein (Abclonal, catalog RP01260). Simple Western quantification of S protein per particle (grey bars). S-protein concentrations in the sample was divided by the particle count and normalized to clone A lot 1 for ease of comparison. Error bars indicate standard deviations from duplicate measurements from a single run using a validated method.

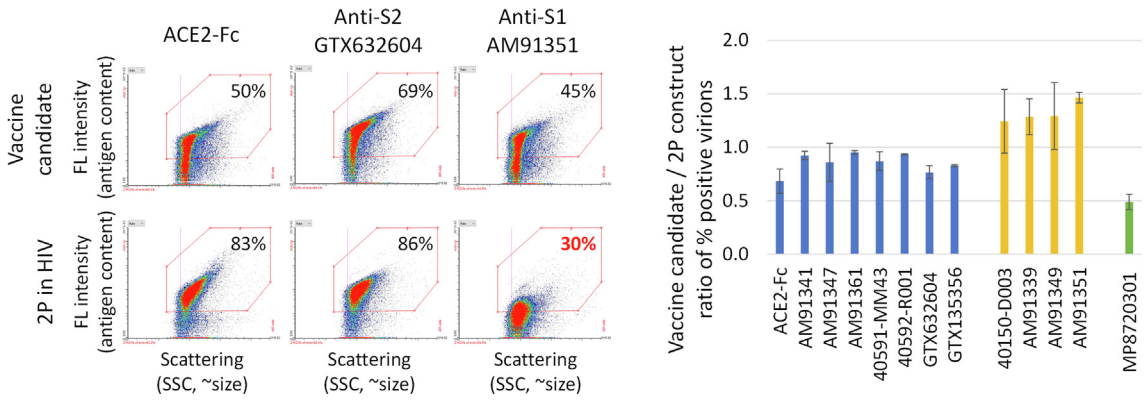

Fig. 4. Comparison of S protein antigenicity by binding studies. Left panel – representative examples of flow virometry data showing reactivity of two S-protein constructs with ACE2-Fc, anti-S2, and anti-S1 antibodies. Right panel – the ratio between the % positive particles in the vaccine candidate and the 2P construct. The x-axis indicates catalog numbers of antibodies used. Error bars indicate standard deviations from duplicate independent runs.

bar). This result therefore suggests that there are differences in epitopes between the variants. While it is not possible to understand the nature of such differences from this experiment, the relatively rapid screen performed by flow virometry can identify such differences, which can be further interrogated by other methods. Flow virometry can therefore be a useful screening tool to evaluate antigen conformation during the discovery phase. It is also possible that a conformational change could have occurred when the protein was expressed on HIV-1 pseudoparticles versus VSV virions. While we did not explore this hypothesis, in a separate study we compared other S-protein variants expressed either on measles virions or HIV-1 and the expression on these two different pseudoparticles did not affect how the S protein reacted with the panel of antibodies (data not shown, to be described in a separate manuscript).

Binding to a panel of antibodies was also employed to evaluate the impact of virus inactivation on the antigenicity of the S protein (Fig. 5). In order to assess the importance of virus replication for the efficacy of the vaccine candidate, we sought to inactivate the virus in such a way that virus infectivity would be significantly reduced while the epitopes on the S protein would remain intact. To that end, samples were subjected to gamma irradiation (targeting 16 kGy total exposure) and to elevated temperature (7 days at 37 °C or 45 °C) and then measured for virus infectivity and antigenicity. Heat treatment completely abolished infectivity of the sample, while gamma irradiation reduced infectivity by over 5 logs. Heat-treated samples showed a significant reduction in the signal for about half of the antibodies. In contrast, the sample inactivated by gamma irradiation exhibited essentially unchanged reactivity. This data suggested that the gamma-irradiated sample maintained antigenicity better than the heat-treated samples. Similar data were reported when UV irradiation and heat treatment were compared as means for inactivation of SARS-CoV-2 virus itself [22] where reduced antigenicity was observed for heat treated samples relative to samples exposed to UV light.

3.5. S-protein degradation during storage

After approximately one month of sample storage at 4 °C we observed almost complete loss of binding of anti-S1 antibodies, while binding of an anti-S2 antibody remained unchanged (Fig. 6, top panel). Subsequent analysis of the samples by Simple Western revealed that during storage, cleavage of the S protein to S1 and S2 occurred, presumably by a residual protease present in the sample (Fig. 6, bottom panel, left). We hypothesized that the loss of the anti-S1 signal after S1/S2 cleavage seen by flow virometry could be due to dissociation of the S1 subunit as reported by others [12]. To test this hypothesis, we pelleted virus particles by centrifugation and then analyzed the pellet and supernatant by Simple Western for the presence of both S protein subunits using anti-S1 and anti-S2 primary antibodies (Fig. 6, bottom panel, right). The analysis of two sample lots showed that the S2 subunit remained

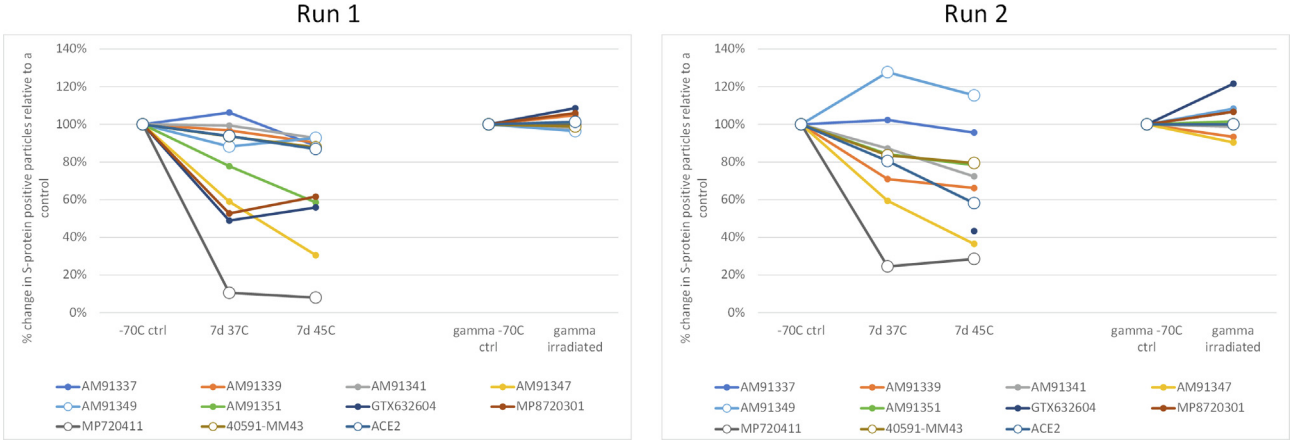

Fig. 5. Impact of heat treatment and gamma irradiation on the antigenicity of S protein. Treatment conditions are indicated on the x-axis. Neutralizing antibodies are indicated with open symbols. Duplicate independent runs are pictured.

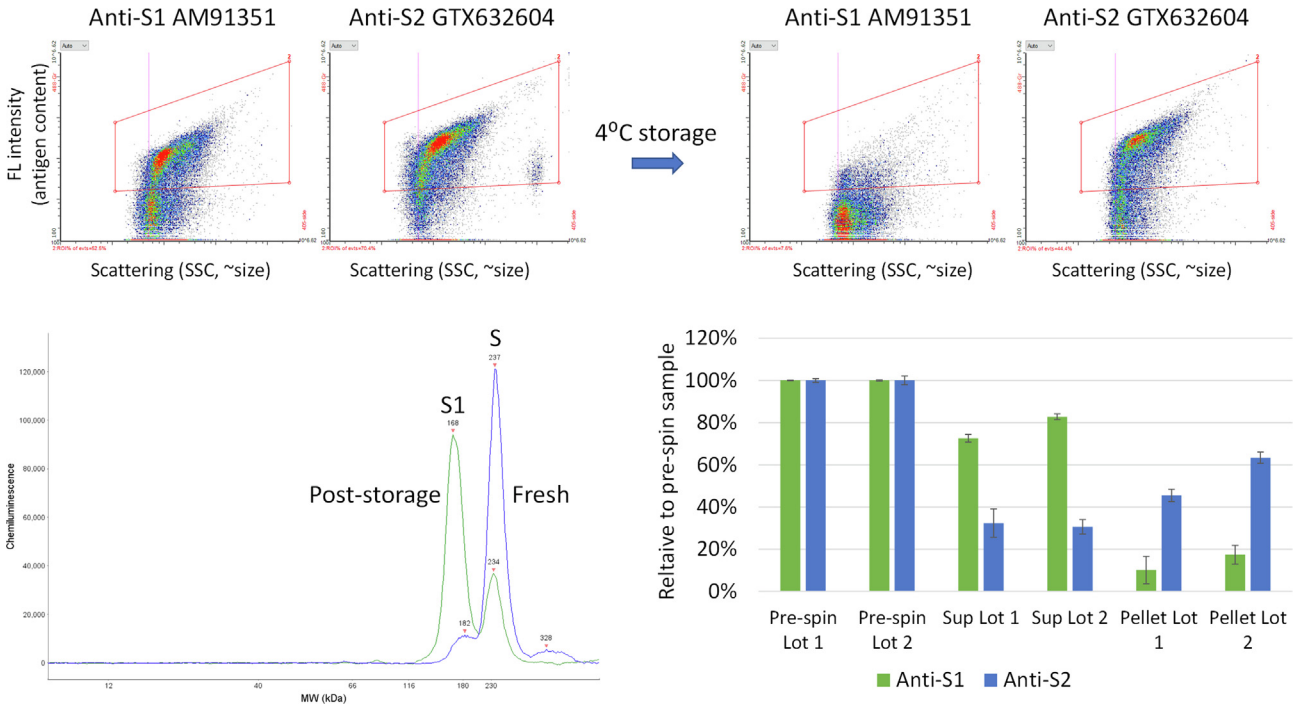

Fig. 6. S1 dissociation from virions after one month of 4 °C storage. Top panel – flow virometry of a sample before and after approximately one month of 4°C storage, labeled with anti-S1 and anti-S2 antibodies. Bottom panel – example anti-S1 Simple Western electropherogram overlay of a sample fresh versus post-storage (left). Peak areas were used for relative S1 and S2 quantitation (using anti-S1 or anti-S2 antibodies) between the supernatant and pellet, then normalized to the sample before centrifugation (right). Data from two lots are shown; error bars indicate standard deviations from duplicate measurements in a single run.

associated with virus particles, however, the S1 subunit was present predominantly in the supernatant, confirming that S1/S2 cleavage has led to dissociation of S1 from the virions.

4. Conclusions

Flow virometry has proven to be a valuable tool to characterize antigens and epitopes presented on the surface of virus particles. Throughout discovery and early preclinical phase of development of a recombinant VSV virus expressing SARS-CoV-2 S protein we used flow virometry to (1) explore the presence of the S protein on virus particles and provide relative antigen quantification between samples with varying expression, (2) assess binding differences of sequence variants with a panel of monoclonal antibodies, (3) evaluate changes in the antigen after virus inactivation either by exposure to high temperature or by gamma irradiation, and (4) observe antigen degradation during storage. Collectively, flow virometry provided important data that helped to guide decisions during vaccine development.

Owing to the unprecedented effort of the scientific community in Covid 19 research, many monoclonal antibodies and other reagents related to SARS-CoV-2 research are commercially available, which greatly facilitated this work. However, this is often not the case for other diseases and significant resources need to be dedicated to in-house development of antibodies and their characterization [23].

Declaration of Competing Interest

The authors declare the following financial interests/personal relationships which may be considered as potential competing interests: Josef Vlasak reports financial support was provided by US Department of Health and Human Services.

Acknowledgements

We want to thank Erica Strable and Aimin Tang for preparing the heat treated and gamma irradiated samples, respectively; Andrew Bett for helpful discussions; Yanjie Wang for process testing support; and Anne Payne, Daisy Richardson, and Malini Mukherjee for their help in reviewing of the manuscript. This project has been funded in part with federal funds from the Department of Health and Human Services; Office of the Assistant Secretary for Preparedness and Response; Biomedical Advanced Research and Development Authority, under Contract No. HHSO100201600031C.

References

[1] Lippé R, Glaunsinger BA. Flow virometry: a powerful tool to functionally characterize viruses. J Virol 2018;92(3).
[2] Nolan JP. Flow cytometry of extracellular vesicles: potential, pitfalls, and prospects. Curr Protocols Cytometry 2015;73(1).
[3] Vlasak J, Hoang VM, Christanti S, Peluso R, Li F, Culp TD. Use of flow cytometry for characterization of human cytomegalovirus vaccine particles. Vaccine 2016;34(20):2321–8.
[4] Renner TM, Tang VA, Burger D, Langlois M-A, Simon V. Intact viral particle counts measured by flow virometry provide insight into the infectivity and genome packaging efficiency of Moloney Murine Leukemia Virus. J Virol 2020;94(2).
[5] Zicari S, Arakelyan A, Fitzgerald W, Zaitseva E, Chernomordik LV, Margolis L, et al. Evaluation of the maturation of individual Dengue virions with flow virometry. Virology 2016;488:20–7.
[6] Landowski M, Dabundo J, Liu Q, Nicola AV, Aguilar HC, Lyles DS. Nipah virion entry kinetics, composition, and conformational changes determined by enzymatic virus-like particles and new flow virometry tools. J Virol 2014;88(24):14197–206.
[7] Arakelyan A, Fitzgerald W, King DF, Rogers P, Cheeseman HM, Grivel J-C, et al. Flow virometry analysis of envelope glycoprotein conformations on individual HIV virions. Sci Rep 2017;7(1).
[8] Staropoli I, Dufloo J, Ducher A, Commere P-H, Sartori-Rupp A, Novault S, et al. Flow Cytometry Analysis of HIV-1 Env Conformations at the Surface of Infected Cells and Virions: Role of Nef, CD4, and SERINC5. J Virol 2020;94(6).

[9] Teo SP. Review of COVID-19 mRNA Vaccines: BNT162b2 and mRNA-1273. J Pharm Pract 2021;8971900211009650.
[10] Krammer F. SARS-CoV-2 vaccines in development. Nature 2020;586 (7830):516–27.
[11] Bosch BJ, van der Zee R, de Haan CAM, Rottier PJM. The coronavirus spike protein is a class I virus fusion protein: structural and functional characterization of the fusion core complex. J Virol 2003;77(16):8801–11.
[12] Cai Y, Zhang J, Xiao T, Peng H, Sterling SM, Walsh RM, et al. Distinct conformational states of SARS-CoV-2 spike protein. Science 2020;369 (6511):1586–92.
[13] Dejnirattisai W, Zhou D, Ginn HM, Duyvesteyn HME, Supasa P, Case JB, et al. The antigenic anatomy of SARS-CoV-2 receptor binding domain. Cell 2021;184 (8):2183–2200.e22.
[14] Liu L, Wang P, Nair MS, Yu J, Rapp M, Wang Q, et al. Potent neutralizing antibodies against multiple epitopes on SARS-CoV-2 spike. Nature 2020;584 (7821):450–6.
[15] Wrapp D, Wang N, Corbett KS, Goldsmith JA, Hsieh C-L, Abiona O, et al. Cryo-EM structure of the 2019-nCoV spike in the prefusion conformation. Science 2020;367(6483):1260–3.
[16] Walls AC, Park Y-J, Tortorici MA, Wall A, McGuire AT, Veesler D. Structure, Function, and Antigenicity of the SARS-CoV-2 Spike Glycoprotein. Cell 2020;181(2):281–292.e6.
[17] Papa G, Mallery DL, Albecka A, Welch LG, Cattin-Ortolá J, Luptak J, et al. Furin cleavage of SARS-CoV-2 Spike promotes but is not essential for infection and cell-cell fusion. PLoS Pathog 2021;17(1):e1009246.
[18] Pallesen J, Wang N, Corbett KS, Wrapp D, Kirchdoerfer RN, Turner HL, et al. Immunogenicity and structures of a rationally designed prefusion MERS-CoV spike antigen. Proc Natl Acad Sci USA 2017;114(35).
[19] Caulfield MJ, Wang Su, Smith JG, Tobery TW, Liu Xu, Davies M-E, et al. Sustained peptide-specific gamma interferon T-cell response in rhesus macaques immunized with human immunodeficiency virus gag DNA vaccines. J Virol 2002;76(19):10038–43.
[20] Ge P, Tsao J, Schein S, Green TJ, Luo M, Zhou ZH. Cryo-EM model of the bullet-shaped vesicular stomatitis virus. Science 2010;327(5966):689–93.
[21] Ricci G, Minsker K, Kapish A, Osborn J, Ha S, Davide J, et al. Flow virometry for process monitoring of live virus vaccines-lessons learned from ERVEBO. Sci Rep 2021;11(1).
[22] Loveday EK, Hain KS, Kochetkova I, Hedges JF, Robison A, Snyder DT, et al. Effect of Inactivation Methods on SARS-CoV-2 Virion Protein and Structure. Viruses 2021;13(4):562.
[23] Ha S, Li F, Troutman MC, Freed DC, Tang A, Loughney JW, et al. Neutralization of Diverse Human Cytomegalovirus Strains Conferred by Antibodies Targeting Viral gH/gL/pUL128-131 Pentameric Complex. J Virol 2017;91(7).